NASA TECHNICAL NOTE

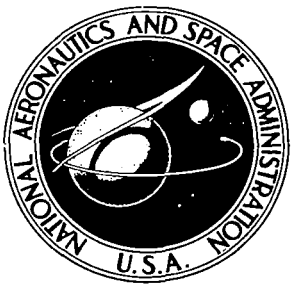

NASA TN D-6509

NASA TN D-6509

EXPLORATORY WIND-TUNNEL INVESTIGATION OF DEPLOYABLE FLEXIBLE VENTRAL FINS FOR USE AS AN EMERGENCY SPIN-RECOVERY DEVICE

by Sanger M. Burk, Jr.

Langley Research Center
Hampton, Va. 23365

NATIONAL AERONAUTICS AND SPACE ADMINISTRATION • WASHINGTON, D. C. • OCTOBER 1971

1. Report No.	2. Government Accession No.	3. Recipient's Catalog No.
NASA TN D-6509		

4. Title and Subtitle	5. Report Date
EXPLORATORY WIND-TUNNEL INVESTIGATION OF DEPLOYABLE FLEXIBLE VENTRAL FINS FOR USE AS AN EMERGENCY SPIN-RECOVERY DEVICE	October 1971
	6. Performing Organization Code
7. Author(s)	8. Performing Organization Report No.
Sanger M. Burk, Jr.	L-7877
	10. Work Unit No.
9. Performing Organization Name and Address	136-62-02-03
NASA Langley Research Center Hampton, Va. 23365	11. Contract or Grant No.
	13. Type of Report and Period Covered
12. Sponsoring Agency Name and Address	Technical Note
National Aeronautics and Space Administration Washington, D.C. 20546	14. Sponsoring Agency Code

15. Supplementary Notes

Technical Film Supplement L-1103 available on request.

16. Abstract

Spin-tunnel tests have been conducted on dynamic models of two fighter airplanes to explore the feasibility of using deployable flexible ventral fins as an emergency spin-recovery device. Various fin configurations, deflections, and locations were tested. The results indicated that the fins provided satisfactory spin recoveries for the models tested.

17. Key Words (Suggested by Author(s))	18. Distribution Statement
Aircraft safety Spin tests Wind tunnel models Recovery device Spin recovery device (suggested term)	Unclassified – Unlimited

19. Security Classif. (of this report)	20. Security Classif. (of this page)	21. No. of Pages	22. Price*
Unclassified	Unclassified	33	$3.00

*For sale by the National Technical Information Service, Springfield, Virginia 22151

EXPLORATORY WIND-TUNNEL INVESTIGATION OF DEPLOYABLE FLEXIBLE VENTRAL FINS FOR USE AS AN EMERGENCY SPIN-RECOVERY DEVICE

By Sanger M. Burk, Jr.
Langley Research Center

SUMMARY

An investigation has been conducted in the Langley spin tunnel to explore the effectiveness of deployable flexible ventral fins as an emergency spin-recovery device. Various configurations, deflections, and locations of the ventral fins were tested on 1/30- and 1/40-scale dynamic models representing two different fighter airplanes. Recoveries were attempted only from fast flat spins, which are the most difficult type from which to recover. Brief supplementary static force tests were conducted on a larger version of one of the models to aid in the explanation of some of the spin-tunnel results. The results of the dynamic free-spinning tests indicated that such deployable flexible ventral fins could consistently give satisfactory spin recoveries for the models tested.

INTRODUCTION

The armed services require a contractor to demonstrate by full-scale flight tests the spin-recovery characteristics of fighter and trainer airplanes as a standard part of the flight-demonstration acceptance program (refs. 1 and 2). During these full-scale spin demonstrations, the airplane is equipped with an emergency spin-recovery device, usually a tail-mounted parachute, in case the spin cannot be terminated by use of the aircraft control surfaces. Although the parachute is the most extensively used emergency spin-recovery device, it has some serious disadvantages. For example, the parachute can be affected adversely by the wake of the airplane. Also, at the same time that the parachute produces an antispin yawing moment, it produces a nose-down pitching moment which may retard the spin recovery of certain types of airplanes. Finally, once the parachute is deployed it cannot be used again during the same flight. The Air Force has indicated in reference 3 that it would be desirable to have a system that could be retracted and used again during the same flight.

In an effort to find a more suitable spin-recovery device, an exploratory investigation has been conducted in the Langley spin tunnel to study the feasibility of using deployable flexible ventral fins as a recovery device. Small fixed ventral fins have been used

effectively on light personal-owner-type airplanes to improve the spin-recovery characteristics (ref. 4), but because their size is limited by ground-clearance requirements, ventral fins generally are ineffective on fighter and attack airplanes. Deployable ventral fins made of rigid materials would also be subject to size limitations because they would have to be retracted. It would seem to be possible to overcome these size limitations by application, or adaptation, of the technology developed over the past few years for deployable flexible wings, and thus to deploy a ventral fin of sufficient size to cause an airplane to recover from a spin. Advantages of such a fin are that it (1) does not operate in the aircraft wake, (2) deploys positively by mechanical means, (3) applies primarily an antispin yawing moment for recovery, (4) applies a relatively small pitching moment as compared with a tail-mounted parachute, and (5) is reusable. It is recognized that the problems of designing and installing this type of recovery system would probably be somewhat greater than those of a comparable spin-recovery parachute system, and the ventral fin system would be heavier and require more volume for storage.

Since the fast flat spin is the most difficult to terminate, and is consequently the critical case, the ventral fins were tested on two different dynamic models exhibiting such a flat spin. These models had their mass distributed primarily along the fuselage (fuselage-heavy loaded), which is characteristic of modern fighter airplanes. Various configurations, deflections, and locations of ventral fins were tested on the dynamic models. Also, brief force tests were conducted on a larger static model of one of the configurations to help explain some of the spin-tunnel results.

SYMBOLS

The longitudinal and lateral force-test data are referred to the body-axis system, as shown in figure 1. The data are presented with respect to the 33.9-percent point of the mean aerodynamic chord of the wing. The physical quantities in this paper are given in the International System of Units with the U.S. Customary Units in parentheses. The measurements and calculations were made in U.S. Customary Units. Factors relating the two systems are given in reference 5.

b	wing span, m (ft)
c	local wing chord, cm (in.)
$\bar{c}$	mean aerodynamic chord, m (ft)
C_A	axial-force coefficient, $\frac{\text{Axial force}}{qS}$

C_l rolling-moment coefficient, $\frac{\text{Rolling moment}}{qSb}$

C_m pitching-moment coefficient, $\frac{\text{Pitching moment}}{qS\bar{c}}$

C_N normal-force coefficient, $\frac{\text{Normal force}}{qS}$

C_n yawing-moment coefficient, $\frac{\text{Yawing moment}}{qSb}$

C_Y lateral-force coefficient, $\frac{\text{Lateral force}}{qS}$

d distance from center of gravity ($0.339\bar{c}$) of dynamic model A or static model A to trailing edge of base chord of ventral fin (see fig. 13(a)), m (ft)

I_X, I_Y, I_Z moment of inertia about X, Y, and Z body axis, respectively, kg-m^2 (slug-ft^2)

$\frac{I_X - I_Y}{mb^2}$ inertia yawing-moment parameter

$\frac{I_Y - I_Z}{mb^2}$ inertia rolling-moment parameter

$\frac{I_Z - I_X}{mb^2}$ inertia pitching-moment parameter

l overall length of dynamic model A or static model A, m (ft)

m mass of airplane, kg (slugs)

q free-stream dynamic pressure, N/m^2 (lb/ft^2)

S wing area, m^2 (ft^2)

V vertical component of resultant velocity (rate of descent), m/sec (ft/sec)

V_R resultant linear velocity (relative wind), m/sec (ft/sec)

X,Y,Z airplane body axes (fig. 1)

x distance from leading edge of mean aerodynamic chord to center of gravity, m (ft)

z distance between center of gravity and fuselage reference line (positive when center of gravity is below line), m (ft)

α_d angle between fuselage reference line of dynamic model and the vertical (approximately equal to absolute value of angle of attack at plane of symmetry), deg

α_s angle between fuselage reference line of static model and the horizontal, deg

β angle of sideslip at tail of model; in a right spin the sideslip at the tail is negative (see fig. 2), deg

Δ increment of coefficient produced by addition of ventral fins to model alone with the controls set in a prospin condition

δ_f deflection of ventral fins, measured from plane of symmetry of model; in a right erect spin δ_f is positive when fin is deflected to pilot's right, and in a left erect spin δ_f is positive when fin is deflected to pilot's left (see fig. 2), deg

μ airplane relative-density coefficient, $m/\rho Sb$

ρ air density, kg/m^3 ($slugs/ft^3$)

ϕ angle between Y body axis and the horizontal, measured in vertical plane, deg

Ω angular velocity about spin axis, revolutions per second

MODELS

Dynamic Models

The dynamic models used in the present investigation were 1/30- and 1/40-scale models representing two different fighter-type airplanes and will, hereafter, be referred

to as models A and B, respectively. A three-view drawing of model A is presented in figure 3; a similar drawing of model B, which has a variable-sweep wing, is presented in figure 4. The dimensional characteristics of the airplane represented by model A are presented in table I and those of the airplane represented by model B are presented in table II. Model A was ballasted to obtain dynamic similarity to the airplane at an altitude of 7620 m (25 000 ft), and model B was ballasted for an altitude of 9144 m (30 000 ft). The full-scale mass characteristics and inertia parameters of the airplanes represented by models A and B are presented in table III.

The deployable ventral fins were triangular and consisted of light, nonporous fabric glued to a framework of spring-tempered wire 0.16 cm (1/16 in.) in diameter. The construction of a typical ventral fin is shown in figure 5. The wire framework was formed in the shape of an acute angle with a loop at the apex to provide the flexibility required for retraction. Two types of ventral fins were used – single, as illustrated in figure 5, and inverted-V, as illustrated in figure 6. The single fins were tested in large, intermediate, and small sizes (see fig. 7) and the inverted-V fins in the large and small sizes. A photograph of model B with the large single ventral fin deployed is shown in figure 8. A spreader bar was added to the framework of the large and intermediate ventral fins to provide further stiffness for a few tests so as to reduce fabric curvature under load. The bar, which was powered by a rubber band, spread and locked the ventral fin at an angle of 50° as illustrated in figure 9.

Static Model

The static force tests were conducted on an existing model which was identical to model A except that it was 1/11 scale and incorporated some tail modifications. The anhedral of the horizontal tail of the 1/11-scale model was 23° rather than 15° and the fuselage had been extended slightly at the tail to accommodate a spin-recovery parachute and a drag-brake parachute. A three-view drawing and a photograph of the model are shown in figures 10 and 11, respectively.

A nondeployable scaled-up version of the large single ventral fin used on dynamic model A was used in the static force investigation. The construction of the ventral fin is shown in figure 12. Fabric of the same type as used for the dynamic-model fins was glued to two structural members forming the fin – the lower member consisting of a metal tube 1.27 cm (1/2 in.) in diameter and the upper member consisting of a T-shaped bracket. A certain amount of slack was allowed in the fabric in order to simulate the curvature of the fabric (due to airload effects) on the deployable fins used on the dynamic models; the proper curvature of the fabric was obtained by reducing the 50° included angle of the laid-out-flat pattern of the fin to 38° and not changing the original fabric area.

TESTS

Dynamic Models

The dynamic-model tests were conducted in the Langley spin tunnel, which is described in reference 6. The tests on models A and B were conducted at dynamic pressures of 185.8 N/m^2 (3.88 lb/ft^2) and 138.8 N/m^2 (2.90 lb/ft^2), respectively, and the corresponding Reynolds numbers based on $\bar{c}$ were approximately 193 000 and 72 000. The recovery characteristics of the models were determined for one loading condition and for erect spins only. Model A was tested for only right spins and model B for only left spins because of asymmetries in the models which made them spin more easily in one direction than the other and thus gave the desired fast flat spin.

The large single ventral fin was tested on model A at various longitudinal locations, referred to as positions I to IV (fig. 13), and with 0° and 10° deflections to the right. With the spreader bar attached to the large single ventral fin, the model was tested only with the fin set at 0° in position II. The large inverted-V fins were tested with an included angle of 40° in position I on the model. The small single and small inverted-V ventral fins were always at the extreme rear of the model fuselage (see fig. 13).

Only limited tests were performed on model B, and the variable-sweep wing was set at 50° for all tests. Large and intermediate single ventral fins were tested with 10° deflection to the left. The fins were equipped with spreader bars and were located as far aft on the fuselage as possible (see fig. 14). Most of the tests were made with the spreader bar powered (by the rubber band), but for a few tests it was unpowered to allow more slack in the fabric.

Since the present program was only an exploratory investigation, the number of tests conducted on the dynamic models was not sufficient to afford a meaningful numerical comparison between different conditions. Consequently, the results are presented for a given ventral-fin configuration only in terms of whether the recoveries are satisfactory or unsatisfactory with regard to meeting a criterion for a four-turn recovery. This criterion is discussed in more detail in a subsequent section of the report.

The models were tested with maximum prospin control deflections, which is standard practice in tests to evaluate an emergency spin-recovery device. These control-surface deflections (measured perpendicular to the hinge lines) were as follows:

	Model A (Right spin)	Model B (Left spin)
Rudder deflection, deg	30 right	7.5 left
Horizontal-tail deflection, deg	0	0
Right-aileron deflection, deg	30 down	8 up
Left-aileron deflection, deg	0	8 down

Static Model

Static force tests were conducted on the 1/11-scale model A in a low-speed wind tunnel with a 3.66-m (12-ft) octagonal test section. The tests were conducted at a dynamic pressure of 154.65 N/m^2 (3.23 lb/ft^2), and the Reynolds number based on $\bar{c}$ was approximately 479 000. The model was supported by a sting in the top of the model, and the forces and moments were measured by a six-component internal strain-gage balance. A photograph of the model mounted in the tunnel is presented in figure 15.

The aerodynamic characteristics of the model were obtained at an angle of attack of 85° (which is representative of the angle for a flat spin) and over a sideslip range from 0° to -30°. The tests were made on the model with and without the large single ventral fin, and with the prospin control settings that were used on the dynamic model. Tests also were conducted to determine the effect of fin location and deflection.

DYNAMIC-MODEL TESTING TECHNIQUE

The standard hand-launch technique (ref. 6) was used to launch the dynamic models with a rotary motion into the vertically rising airstream of the tunnel. After a steady fast flat spin had been established, the ventral fin was deployed. Visual observations and motion pictures were made of the spin and recovery characteristics of the models.

Prior to launch the fabric of the ventral fin was accordion folded, as indicated in figures 5 and 9, for minimum aerodynamic interference when the fin was in the retracted position on the model. A remote-control mechanism released the fin from the retracted position, allowing it to deploy. The fin was prevented from exceeding the desired lateral deflection (because of the force of the airstream) by a string attached between the fin tip and the tip of the outer wing.

Turns for recovery were measured from the time the ventral fin was deployed to the time the spin rotation ceased. The recovery characteristics of the models from the fast flat spins were considered to be satisfactory if consistent and repeatable recoveries could be obtained within approximately four turns. A larger number of turns is considered acceptable for recovery from a flat spin than from a steep spin $\left(4 \text{ as compared with } 2\frac{1}{4}\right)$ because in a flat spin the altitude loss per turn is less. The overall recovery characteristics of the model for a given condition were considered to be satisfactory only if all the spin recoveries from several different tests were satisfactory. As previously mentioned, prospin controls were maintained during the time the ventral fin was deployed so that the spin recovery was due to the ventral-fin action alone. For models with a fuselage-heavy loading (such as those used in the present investigation) and for an assumed right spin, the ventral fin applies an antispin yawing moment $\left(\text{negative } C_n\right)$, a prospin

rolling moment (negative C_l), and a prospin pitching moment (negative C_m). For further details on the effects of mass distribution and moments on spin recoveries, see reference 6.

RESULTS AND DISCUSSION

The information obtained from the dynamic-model tests in the spin tunnel was qualitative in nature and was used only to explore the feasibility of using a flexible ventral fin as an emergency spin-recovery device. Results of brief static force tests are presented to help explain some of the spin-tunnel results obtained with model A. No attempt was made to correct these data for blockage or Reynolds number effects, and therefore the force-test results are presented in terms of incremental values of C_Y, C_n, C_l, and C_m rather than absolute values.

Typical developed-spin data obtained from tests of the dynamic models with the fins retracted are presented in table IV in terms of full-scale values for the airplanes represented by models A and B. A summary of the spin-recovery results of the dynamic-model tests is presented in table V. In brief, the results indicated that recoveries from the critical fast flat spin could be effected by deployment of flexible ventral fins as spin-recovery devices.

Motion-picture film supplement L-1103, showing some typical results of the spin tests of models A and B, has been prepared and is available on loan. A request card form and description of the film are included at the back of this paper.

Model A

Large single ventral fin.- The angular setting and longitudinal location of the large single ventral fin were very important in determining its effectiveness in terminating a spin. For example, deflecting the fin 10° at position I resulted in consistent, satisfactory recoveries, whereas 0° deflection resulted in both satisfactory and unsatisfactory recoveries. Also, moving the fin to more forward locations led to unsatisfactory recoveries.

During a typical satisfactory spin-recovery sequence after deployment of the large single ventral fin, the outer wing (left wing in right spin) rolled down (prospin) approximately 25° during the first turn, the rate of rotation slowed, and the attitude of the model steepened. As the recovery proceeded, the model generally had a small-amplitude rolling oscillation, and when the rotation finally stopped, the model pitched down to a steep dive.

The reason for the better recovery characteristics with the fin deflected is illustrated in figure 16, which indicates the relative wind and the position of the fabric of the fin. There is a sizable sideslip angle at the rear of the model, due mainly to the spin rotation. Because of the aerodynamic load, the fabric of the fin bows out so that for the

undeflected-fin condition much of the fabric is at very low angles of sideslip. In this condition the fin produces little side force and results in a small antispin yawing moment. With the fin deflected, however, all of the fabric is at a much higher angle of sideslip and produces a larger antispin yawing moment.

Quantitative documentation of this reasoning is presented by the force-test results shown in figures 17 and 18. The negative values of sideslip angle shown correspond to the direction of sideslip at the tail in a right spin, values of -5° to -15° being representative of those for the dynamic models during developed spins. The fin is deflected away from the relative wind (as illustrated in fig. 16), and negative values of ΔC_n correspond to an antispin yawing moment. The data in figure 17 show that increasing the fin deflection from 0° to 30° produced larger values of antispin (negative) yawing moment for the usual range of angles of sideslip (-5° to -15°) in spins.

Prospin (negative) rolling-moment increments were obtained at all negative angles of sideslip for all fin deflections (see fig. 17). Also, prospin (negative) pitching-moment increments were obtained in the range of angles of sideslip corresponding to those calculated for the dynamic model. Despite these adverse rolling and pitching increments, the antispin yawing-moment increments were sufficient to produce a satisfactory spin recovery.

The data presented in figure 18 show the expected reduction in increments of antispin yawing moment and prospin rolling and pitching moments resulting from moving the ventral fin forward on the model. The reduction in yawing and pitching moments occurs because of both the decreased moment arm of the fin and the reduced angle of sideslip at the fin (see fig. 2); the reduced rolling moment results from the decreased angle of sideslip.

It was observed during the spin tests that the fabric on the ventral fin became highly curved because of the side load on the fin as the model rotated. In order to determine whether this condition had a significant effect on the recovery characteristics, a spreader bar was added to the fin of the dynamic model to reduce the curvature by putting more spanwise tension in the fabric. The tests with the spreader bar were conducted with the large single ventral fin located at position II and undeflected. Spin recoveries had been marginal for this condition without the spreader bar, and it was believed that the effect of the spreader bar could be detected more easily for this condition. The test results indicated that use of the spreader bar decreased the average number of turns for recovery by approximately one turn, resulting in satisfactory recoveries. Why the addition of the spreader bar to the fin led to improved spin recoveries is not completely understood; the favorable effect may be due in part to the increase in projected planform area of the fin (approximately 24 percent), which would result in an increase in antispin yawing moment. Another possible favorable effect may be the fact that more of the fabric of the fin was at

a higher angle of sideslip when equipped with a spreader bar, and thus a larger antispin yawing moment was produced.

One spin test was made with the ventral fin (no spreader bar) set at -10° (opposite to the normally used deflections) to determine how the spin-recovery characteristics of the model would be affected. This setting was extremely adverse in that when the fin was deployed, the model oscillated violently between angles of attack of 45° and 90° and roll angles of about 45° and -45° before recovering in an inverted dive. It would appear that injury to the pilot might result from these motions. Thus, if the fin is to be actuated so that it can be tilted laterally, extreme care should be taken so that it is not tilted in the wrong direction.

Small single ventral fin.- The small single fin was tested only in a far rearward position. At deflections of either 0° or 10°, this fin resulted in satisfactory spin recoveries, the recoveries being slightly faster when the fin was set at 10°. The results for the 0° fin setting were contrary to those obtained for the larger fin, where a 0° setting resulted in some unsatisfactory recoveries. The greater effectiveness of the small fin at 0° deflection may be due to its increased stiffness because of its smaller size or may be due to the location of the small fin. This effect is in agreement with the results discussed previously, which showed that stiffening the fin (with a spreader bar) resulted in improved recoveries. The motion of the model during the spin-recovery sequence was similar to that of the model with the large fin except that during the first turn the model rolled only to about 10° rather than 25°.

Inverted-V ventral fins.- The results of the spin tests of the single ventral fins without spreader bars indicated that it was desirable to deflect the fins positively for consistent spin recovery (right deflection in right spin and left deflection in left spin). To apply this type of emergency recovery device the pilot or a sensor must determine the direction of the spin rotation, and seemingly the fin deflection would have to be power actuated. In an attempt to eliminate these disadvantages, inverted-V ventral fins were tested on the model. Of course, this type of fin would be heavier and bulkier than a single fin.

Deployment of the large inverted-V fin with an angle of 40° between the fins resulted in satisfactory spin recoveries. The small inverted-V fin with an included angle of 20° was ineffective in terminating the spin; increasing the included angle to 40° improved the effectiveness of the fins slightly in that both satisfactory and unsatisfactory recoveries were obtained instead of only unsatisfactory recoveries. The recovery sequence of the dynamic model with the large and small inverted-V ventral fins attached was similar to the motion of the model when equipped with the large and small single fins, respectively.

Model B

The results of the tests of model B with the large single ventral fin deflected 10^{o} and equipped with a powered spreader bar indicated that satisfactory spin recoveries could be obtained, but with the spreader bar unpowered (equivalent to no spreader bar), the spin recoveries were unsatisfactory. When the model was equipped with an intermediate-size single ventral fin deflected 10^{o} and a powered spreader bar, the spin recoveries were unsatisfactory.

The spin-recovery sequence of the model when equipped with a large single ventral fin and a powered spreader bar was similar to that of model A with the large fin attached except for the sequence after cessation of the spin rotation. At this point, as previously mentioned, model A would pitch down to an erect or inverted dive, whereas model B either pitched down to an erect dive or rolled to an inverted attitude.

CONCLUDING REMARKS

The results of tests with models of two fighter airplanes to explore the feasibility of using deployable flexible ventral fins as an emergency spin-recovery device indicated that such fins can satisfactorily terminate spins of these airplanes. When a single fin was used, improved spin recoveries were obtained by moving the fin rearward, using a spreader bar on the fin, and deflecting the fin in the positive direction (deflected right in a right spin and left in a left spin). Also, satisfactory recoveries were obtained with an inverted-V ventral fin.

Langley Research Center,
National Aeronautics and Space Administration,
Hampton, Va., September 27, 1971.

REFERENCES

1. Anon.: Demonstration Requirements for Airplanes. Mil. Specif. MIL-D-8708B(AS), Jan. 31, 1969.

2. Anon.: Stall/Post-Stall/Spin Flight Test Demonstration Requirements for Airplanes. Mil. Specif. MIL-S-83691 (USAF), Mar. 31, 1971.

3. Anon.: Flying Qualities of Piloted Airplanes. Mil. Specif. MIL-F-8785B(ASG), Aug. 7, 1969.

4. Klinar, Walter J.; and Wilson, Jack H.: Spin-Tunnel Investigation of the Effects of Mass and Dimensional Variations on the Spinning Characteristics of a Low-Wing Single-Vertical-Tail Model Typical of Personal-Owner Airplanes. NASA TN 2352, 1951.

5. Mechtly, E. A.: The International System of Units – Physical Constants and Conversion Factors (Revised). NASA SP-7012, 1969.

6. Neihouse, Anshal I.; Klinar, Walter J.; and Scher, Stanley H.: Status of Spin Research for Recent Airplane Designs. NASA TR R-57, 1960. (Supersedes NACA RM L57F12.)

TABLE I.- DIMENSIONAL CHARACTERISTICS OF AIRPLANE REPRESENTED BY DYNAMIC MODEL A

Overall length	18.36 m (60.24 ft)
Wing:	
Span	11.71 m (38.41 ft)
Area (theoretical)	49.24 m^2 (530.00 ft^2)
Area (including leading-edge extension)	50.01 m^2 (538.34 ft^2)
Root chord (at airplane center line)	716.28 cm (282.00 in.)
Tip chord (theoretical tip)	119.38 cm (47.00 in.)
Mean aerodynamic chord, $\bar{c}$	488.95 cm (192.50 in.)
Distance from leading edge of root chord to leading edge of $\bar{c}$	281.33 cm (110.76 in.)
Aspect ratio	2.82
Taper ratio	0.167
Sweepback of 25-percent-chord line	45.00°
Dihedral inboard of buttock line 406.4 cm (160.0 in.)	0°
Dihedral outboard of buttock line 406.4 cm (160.0 in.)	12.00°
Incidence	1.00°
Airfoil section:	
Root (at airplane center line)	Modified NACA 0006.4-64
Tip (theoretical)	Modified NACA 0003.0-64
Aileron:	
Area (each) rearward of hinge line	1.22 m^2 (13.08 ft^2)
Span (each, from 44.5 percent b/2 to 67.0 percent b/2)	1.33 m (4.35 ft) or 22.5 percent b/2
Inboard end chord (at buttock line 262.23 cm (103.24 in.))	96.04 cm (37.81 in.) or 21.3 percent c
Outboard end chord (at buttock line 394.82 cm (155.44 in.))	87.33 cm (34.38 in.) or 27.6 percent c
Horizontal tail:	
Area (in chord plane)	8.80 m^2 (94.70 ft^2)
Movable area	7.19 m^2 (77.40 ft^2)
Span	5.40 m (17.705 ft)
Aspect ratio	3.30
Taper ratio	0.20
Sweepback of 25-percent-chord line	35.50°
Dihedral	-15.00°
Root chord (at airplane center line)	271.78 cm (107.00 in.)
Tip chord (theoretical)	54.36 cm (21.40 in.)
Airfoil section:	
Root (at airplane center line)	Modified NACA 0003.7-64
Tip (theoretical)	Modified NACA 0003.0-64
Vertical tail:	
Area (theoretical)	6.27 m^2 (67.50 ft^2)
Span	1.94 m (6.375 ft)
Taper ratio	0.227
Root chord	526.16 cm (207.15 in.)
Tip chord	119.63 cm (47.10 in.)
Sweepback of 25-percent-chord line	58.30°
Airfoil section:	
Root	Modified NACA 0004.0-64
Tip	Modified NACA 0002.5-64
Rudder area (rearward of hinge line)	1.03 m^2 (11.07 ft^2)

TABLE II.- DIMENSIONAL CHARACTERISTICS OF AIRPLANE REPRESENTED BY DYNAMIC MODEL B

[All dimensions are based on 16° wing sweep unless otherwise indicated]

Overall length	22.4 m (73.5 ft)
Wing:	
Span	19.2 m (63 ft)
Area	48.8 m^2 (525 ft^2)
Root chord (at airplane center line)	383.2 cm (150.883 in.)
Tip chord	124.5 cm (49 in.)
Mean aerodynamic chord, $\bar{c}$	275.6 cm (108.5 in.)
Distance from leading edge of root chord to leading edge of $\bar{c}$	114.3 cm (45 in.)
Aspect ratio	7.56
Taper ratio	3.08
Dihedral	1°
Incidence	1°
Airfoil section –	
Root	Modified NASA 64A210.68
Tip	NASA 64A209.8
Horizontal tail:	
Total area	37.8 m^2 (407.3 ft^2)
Span	8.94 m (29.33 ft)
Aspect ratio	2.11
Taper ratio	6.897
Sweepback of leading edge	57°30'
Dihedral	-1°
Root chord (at airplane center line)	683.26 cm (269 in.)
Tip chord (theoretical)	99.06 cm (39 in.)
Airfoil section	Biconvex
Vertical tail:	
Area	10.4 m^2 (111.7 ft^2)
Span	2.7 m (8.9 ft)
Taper ratio	2.435
Root chord	542.2 cm (213.47 in.)
Tip chord	222.7 cm (87.67 in.)
Sweepback of leading edge, deg	55
Airfoil section	Biconvex
Rudder area	2.72 m^2 (29.3 ft^2)

Dimensions for all wing sweep angles:

Wing sweep angle, deg	16	26	50	72.5
Span, m (ft)	19.2 (63)	18.1 (59.5)	14.7 (48.3)	9.7 (31.95)
Mean aerodynamic chord, $\bar{c}$, cm (in.)	275.6 (108.5)	278.9 (109.8)	364.7 (143.6)	704.8 (277.5)
Fuselage station at leading edge of $\bar{c}$, cm (in.)	1214.1 (478.0)	1242.1 (489.0)	1243.6 (489.6)	966.7 (380.6)

TABLE III.- MASS CHARACTERISTICS AND INERTIA PARAMETERS OF THE AIRPLANES REPRESENTED BY MODELS A AND B

[Values given are full scale, and moments of inertia are given about the center of gravity]

Airplane represented by	Weight, N (lb)	Center of gravity		Relative density, μ, at –			Moments of inertia, kg-m^2 (slug-ft^2)			Mass parameters		
		$x/\bar{c}$	$z/\bar{c}$	Sea level	7620 m (25 000 ft)	9144 m (30 000 ft)	I_X	I_Y	I_Z	$\frac{I_X - I_Y}{mb^2}$	$\frac{I_Y - I_Z}{mb^2}$	$\frac{I_Z - I_X}{mb^2}$
Model A	160 977 (36 189)	0.339	0.042	23.22	51.80	----	35 397 (26 108)	157 576 (116 222)	178 459 (131 625)	-543×10^{-4}	-93×10^{-4}	636×10^{-4}
Model B	220 836 (49 646)	0.224	0.045	25.57	----	68.24	70 784 (52 208)	404 816 (298 577)	444 970 (328 195)	-685×10^{-4}	-82×10^{-4}	767×10^{-4}

TABLE IV.- DEVELOPED-SPIN CHARACTERISTICS OF DYNAMIC MODELS WITH VENTRAL FINS RETRACTED

[Values given are full scale]

Model	α_d, deg	ϕ, deg	V		Ω, rps
			m/sec	ft/sec	
A	86	[a]1.0	94.8	311	0.55
B	84	[a]3.3	94.2	309	.38

[a]Inner wing up.

TABLE V.- SUMMARY OF DYNAMIC-TEST RESULTS

Model	Ventral-fin configuration	Fin deflection, deg	Included angle of inverted-V fin, deg	Result for fin position[a] –				
				Tail of model	I	II	III	IV
A	Large single	0			U	U		
		10			S	U	U	U
		-10			U			
A	Large single with spreader bar unpowered	0				S		
A	Small single	0		S				
		10		S				
A	Large inverted-V		40		S			
A	Small inverted-V		20	U				
			40	U				
B	Large single with spreader bar	10		S				
B	Large single with spreader bar unpowered	10		U				
B	Intermediate single with spreader bar	10		U				

[a]Fin positions are illustrated in figures 13 and 14. The letter S indicates satisfactory spin recovery; U indicates unsatisfactory spin recovery.

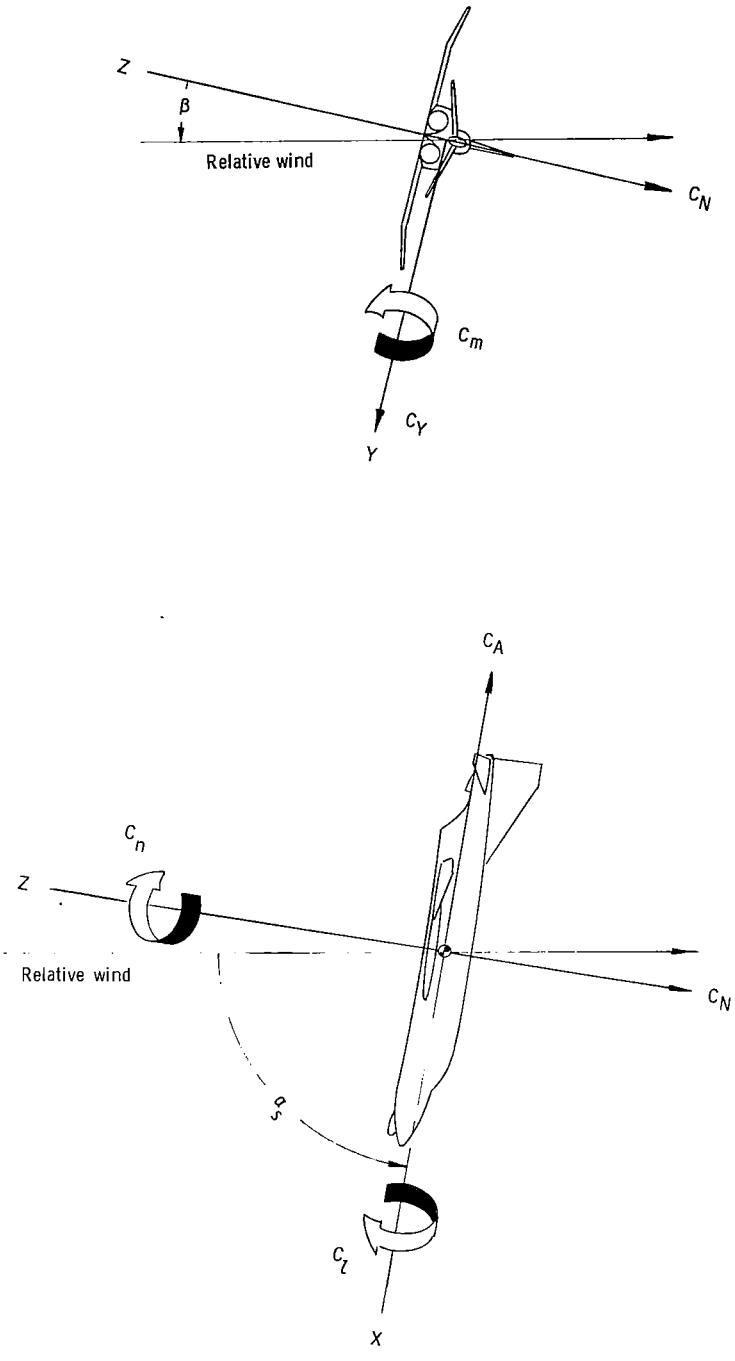

Figure 1.- Body-axis system used for static force-test data. Arrows indicate positive directions of moments, forces, and angles.

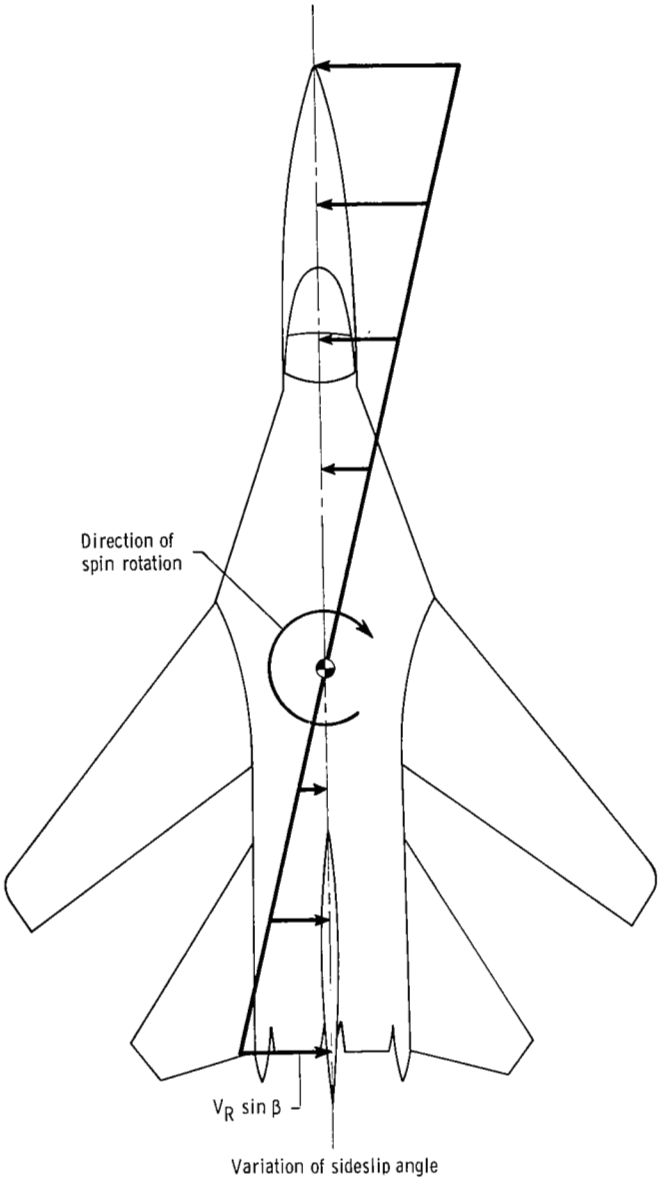

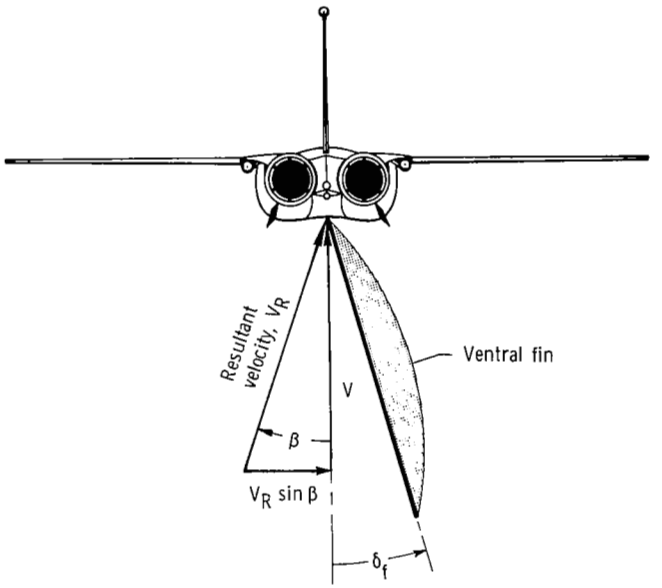

Velocity vector diagram and fin deflection at tail.

Figure 2.- Sideslip generated at aircraft tail during flat spin to the right with ventral fin deflected in direction to oppose spin rotation.

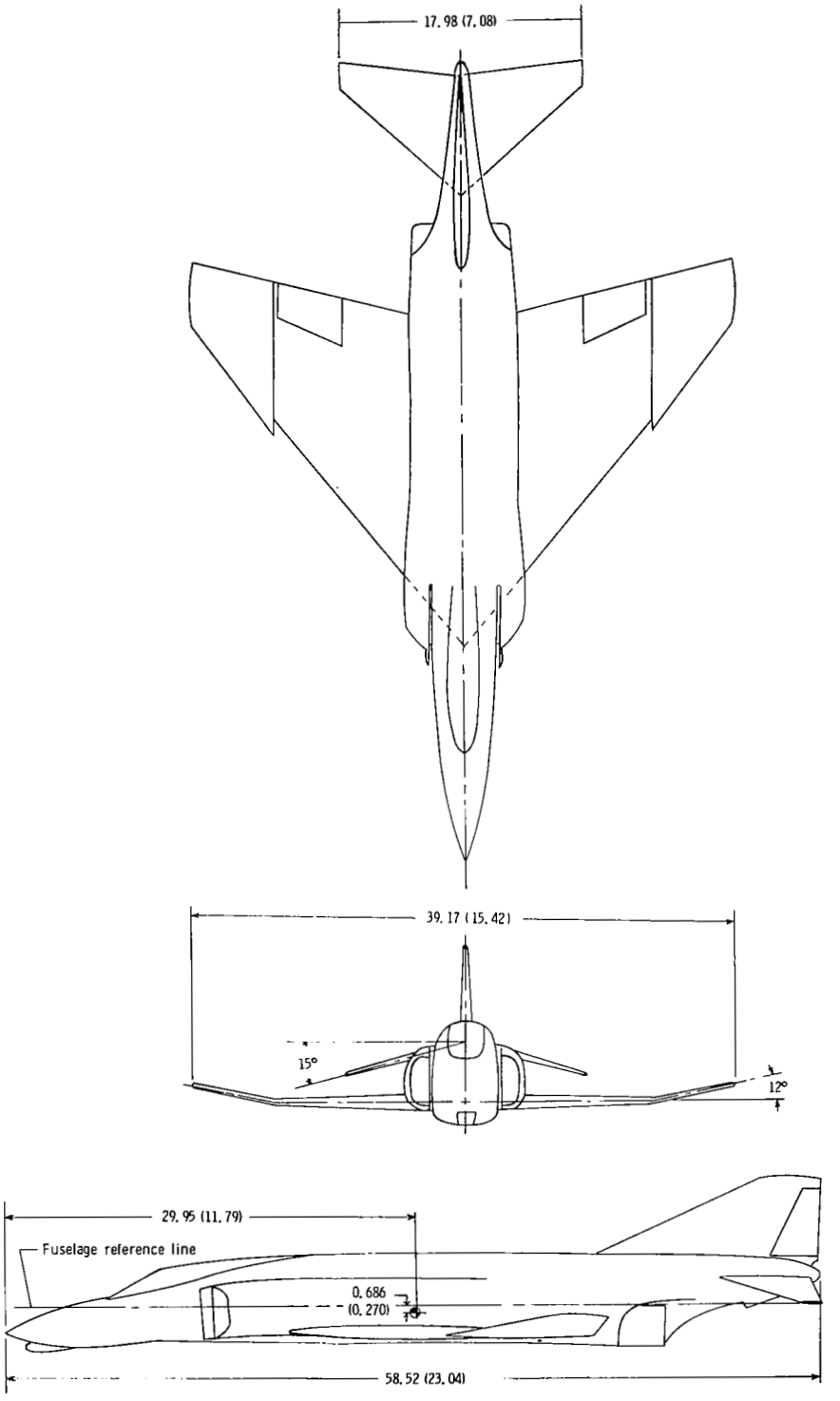

Figure 3.- Three-view drawing of 1/30-scale dynamic model A. Dimensions are in centimeters and parenthetically in inches.

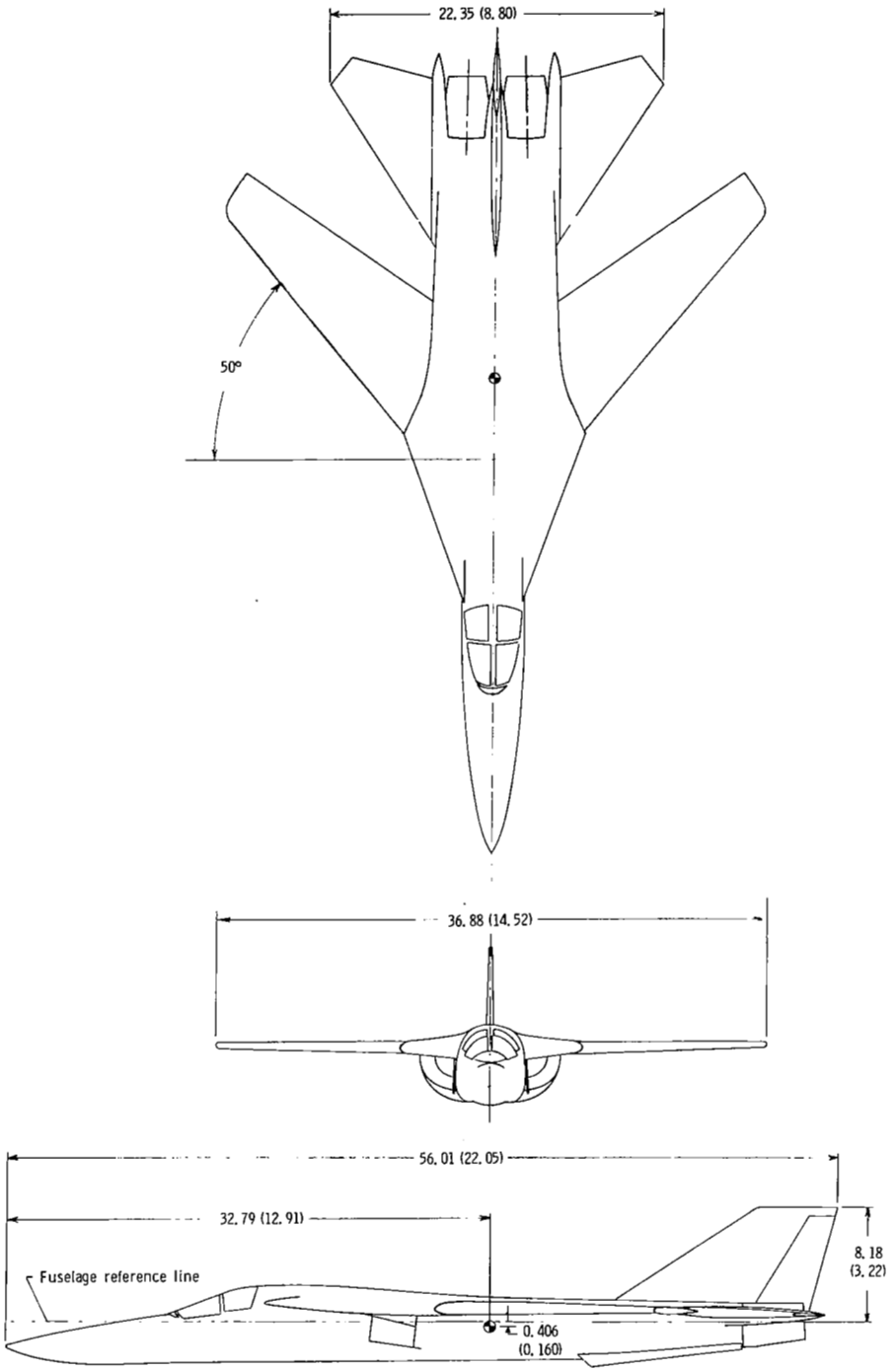

Figure 4.- Three-view drawing of 1/40-scale dynamic model B. Dimensions are in centimeters and parenthetically in inches.

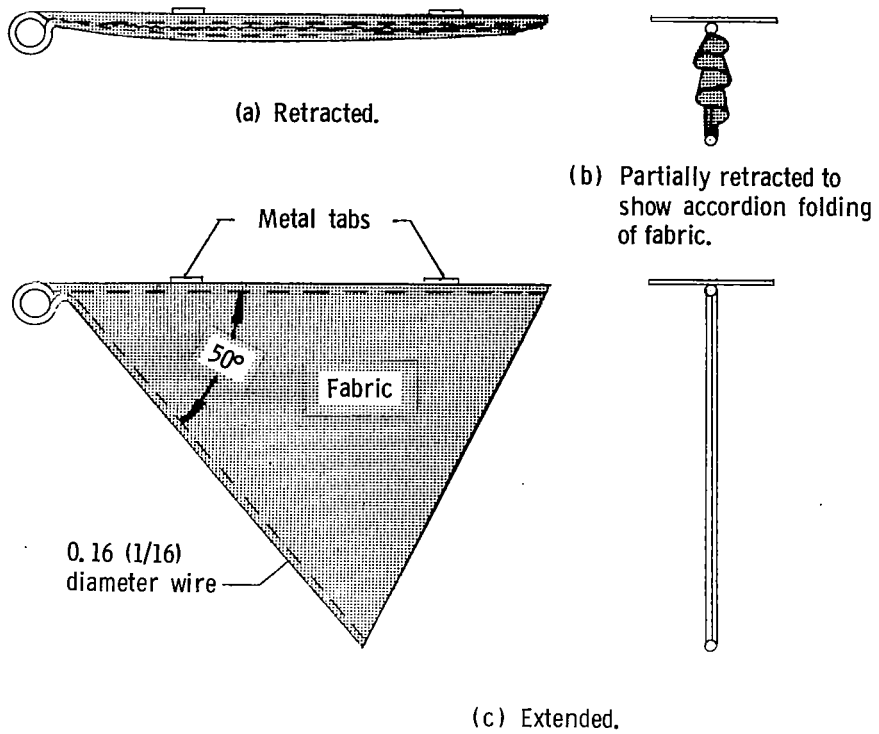

Figure 5.- Construction of typical deployable single ventral fin used on dynamic models. Dimensions are in centimeters and parenthetically in inches.

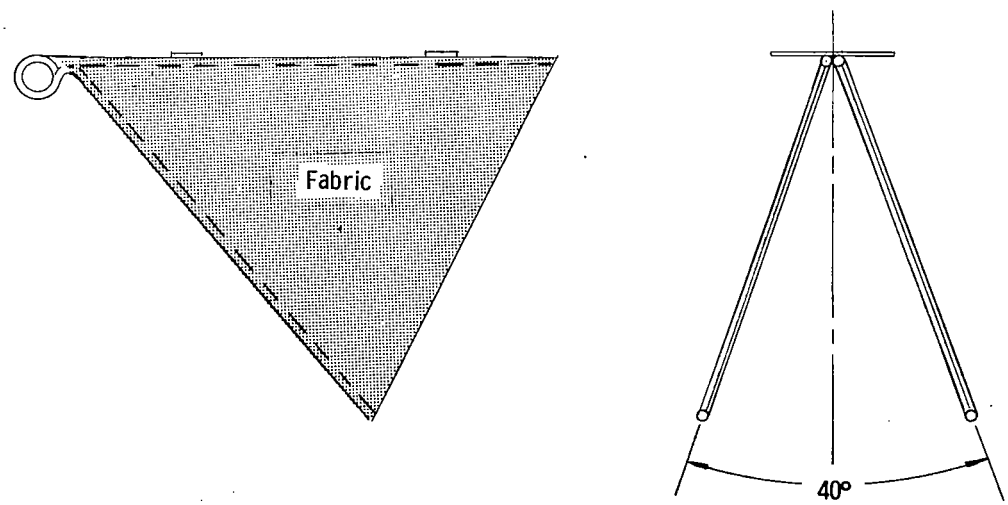

Figure 6.- Typical deployable inverted-V ventral fin used on dynamic model.

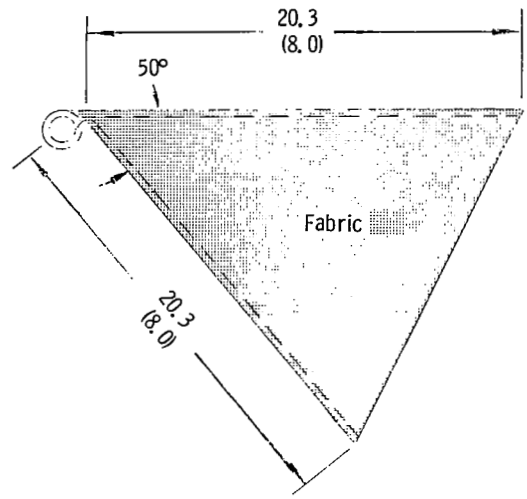

(a) Large.

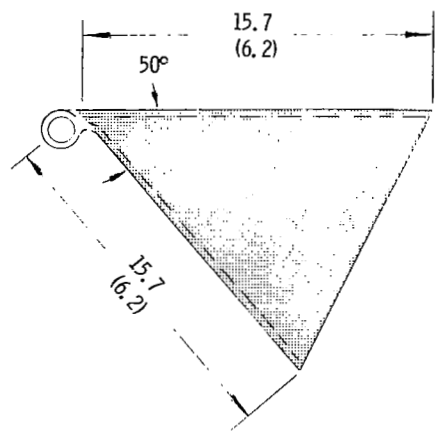

(b) Intermediate.

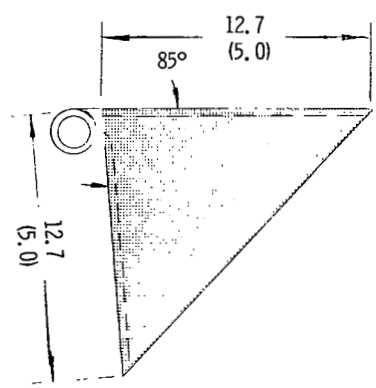

(c) Small.

Figure 7.- Sizes of deployable single ventral fins used on dynamic models. Dimensions are in centimeters and parenthetically in inches.

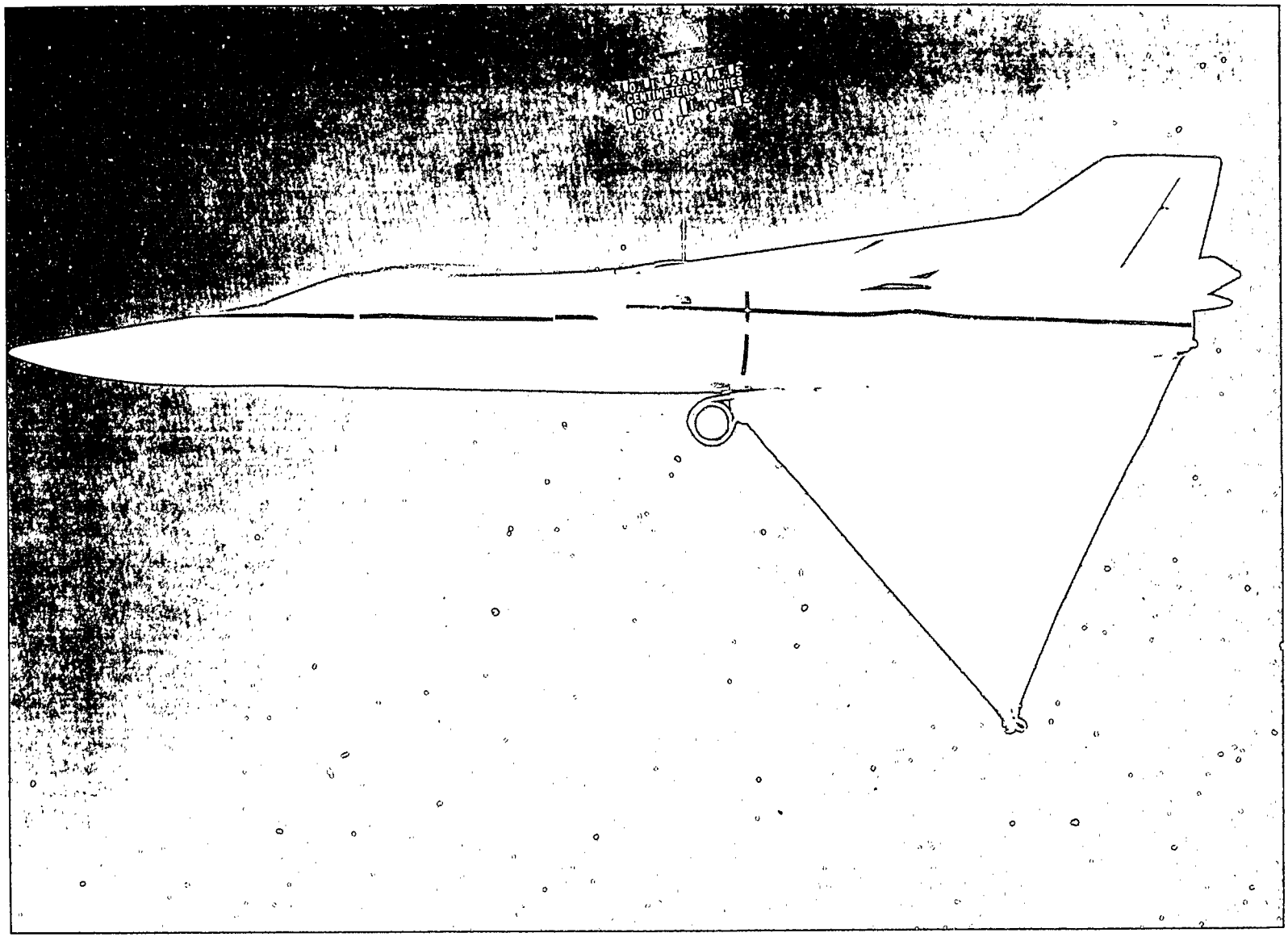

L-70-2698

Figure 8.- The 1/40-scale dynamic model B equipped with a deployable ventral fin.

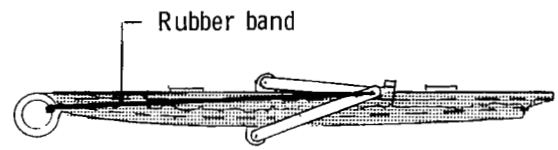

(a) Retracted.

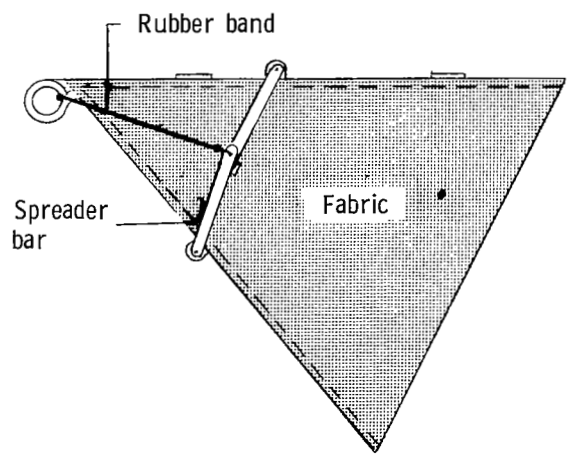

(b) Extended.

Figure 9.- Typical deployable ventral fin equipped with a powered spreader bar.

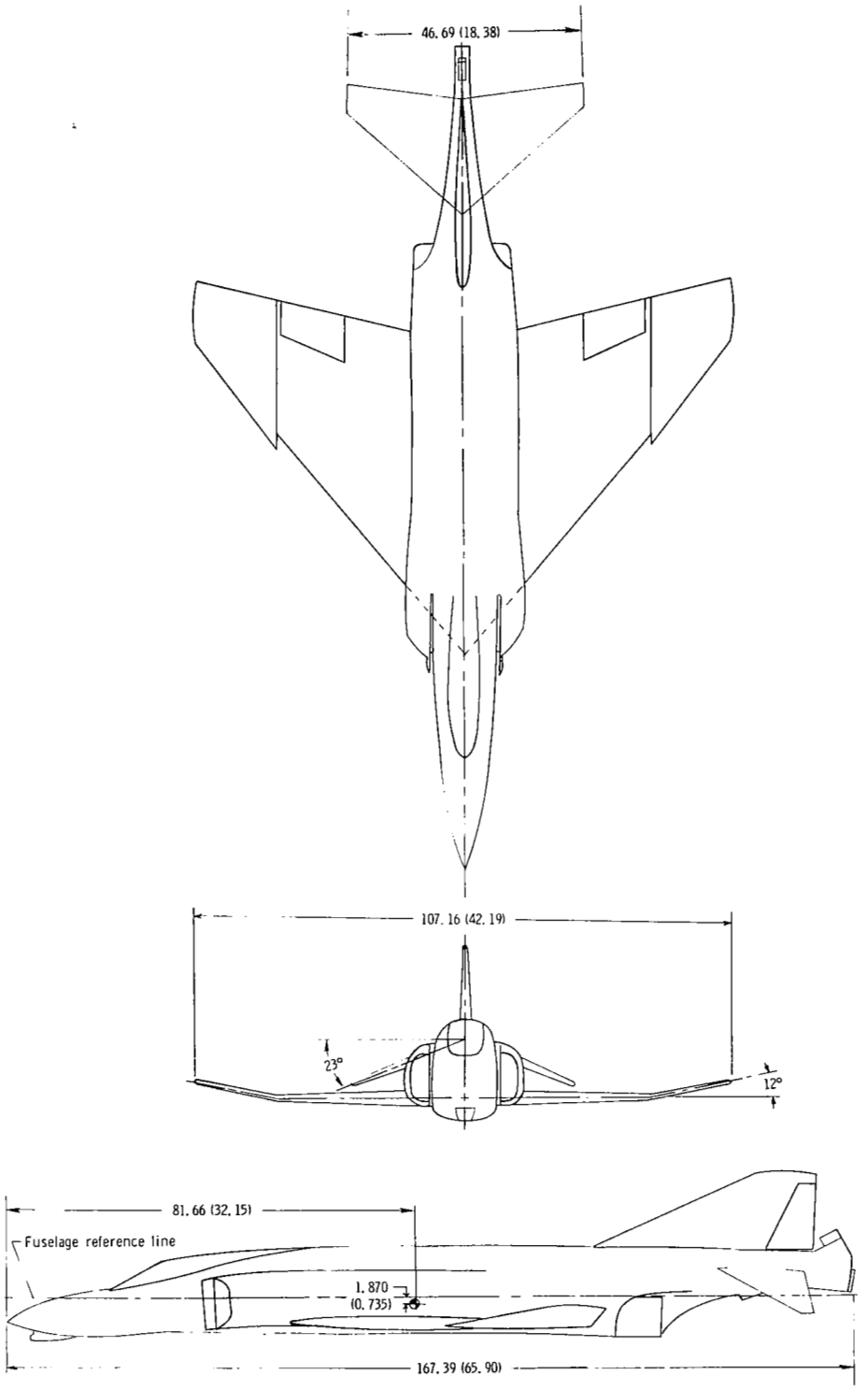

Figure 10.- Three-view drawing of the 1/11-scale static model A. Dimensions are in centimeters and parenthetically in inches.

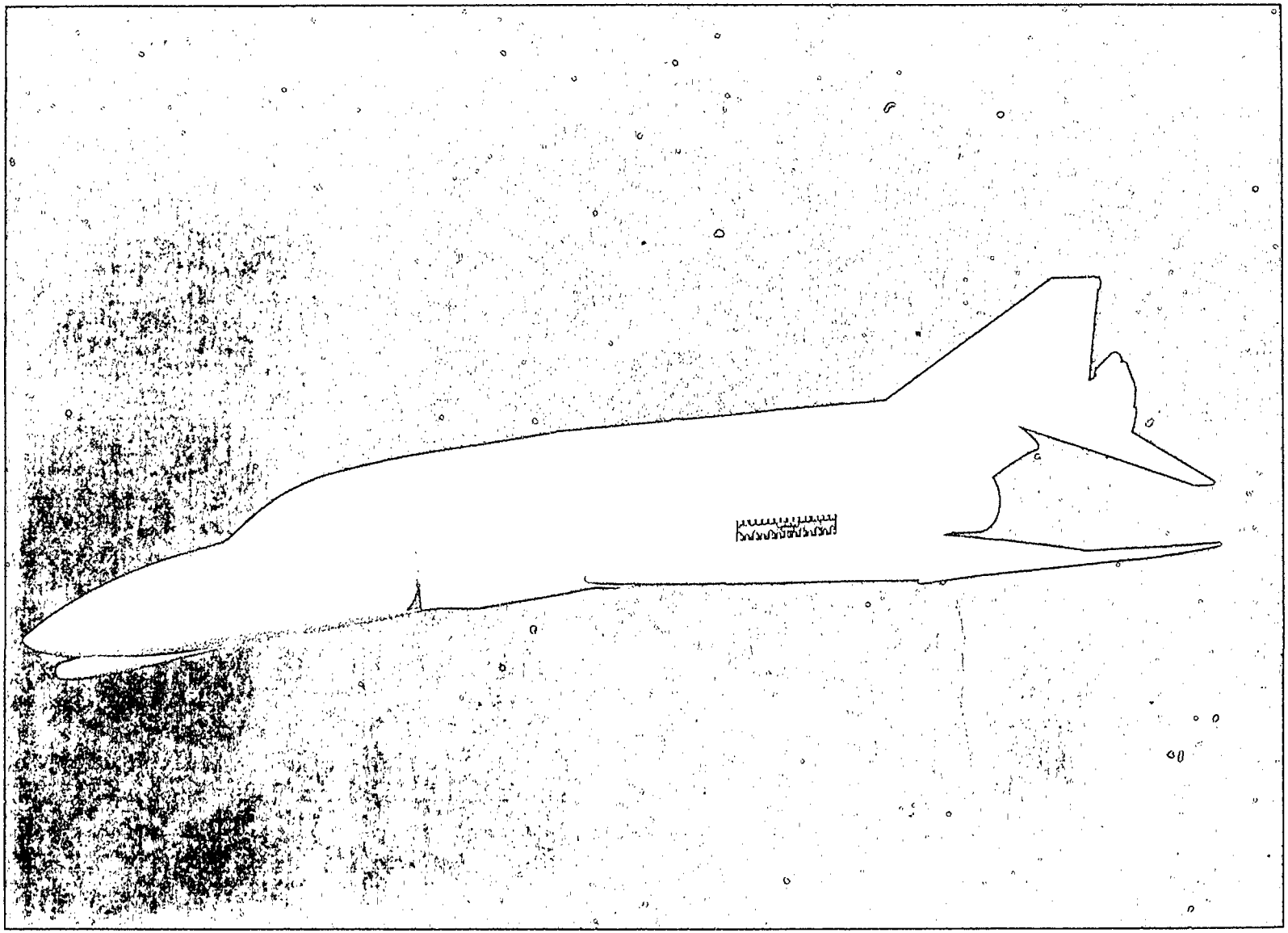

L-69-8494

Figure 11.- The 1/11-scale static model A.

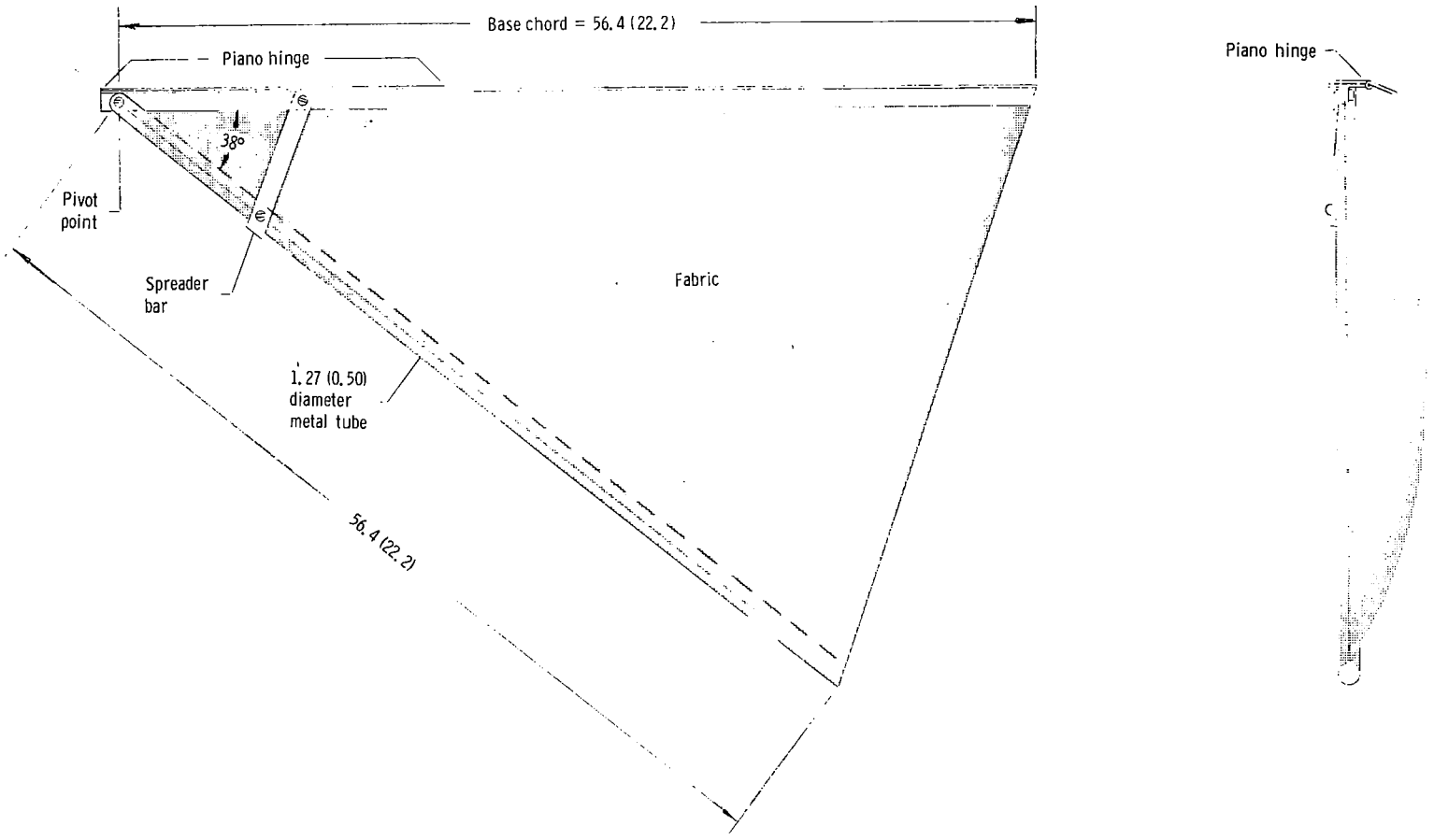

Figure 12.- Construction of typical nondeployable ventral fin used on static model. Dimensions are in centimeters and parenthetically in inches.

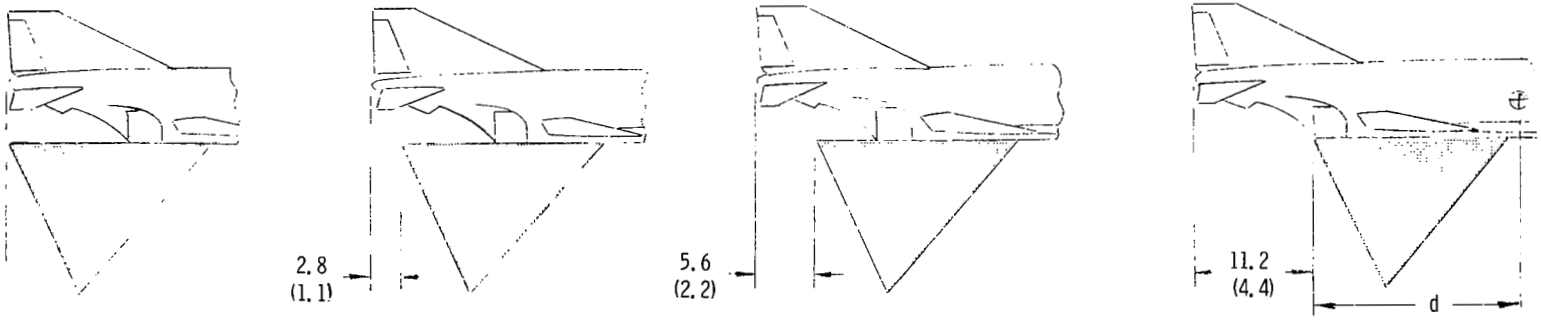

(a) Large ventral fin.

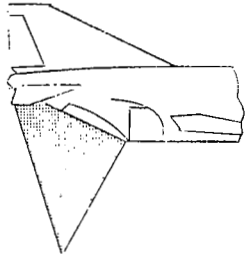

(b) Small ventral fin.

Figure 13.- Locations of single ventral fins tested on dynamic model A. Dimensions are in centimeters and parenthetically in inches.

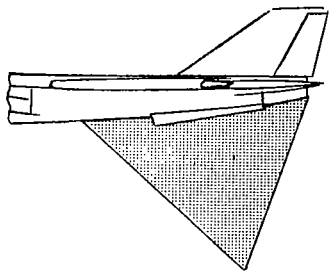

(a) Large ventral fin.

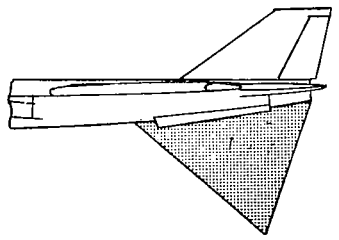

(b) Intermediate ventral fin.

Figure 14.- Locations of single ventral fins tested on dynamic model B.

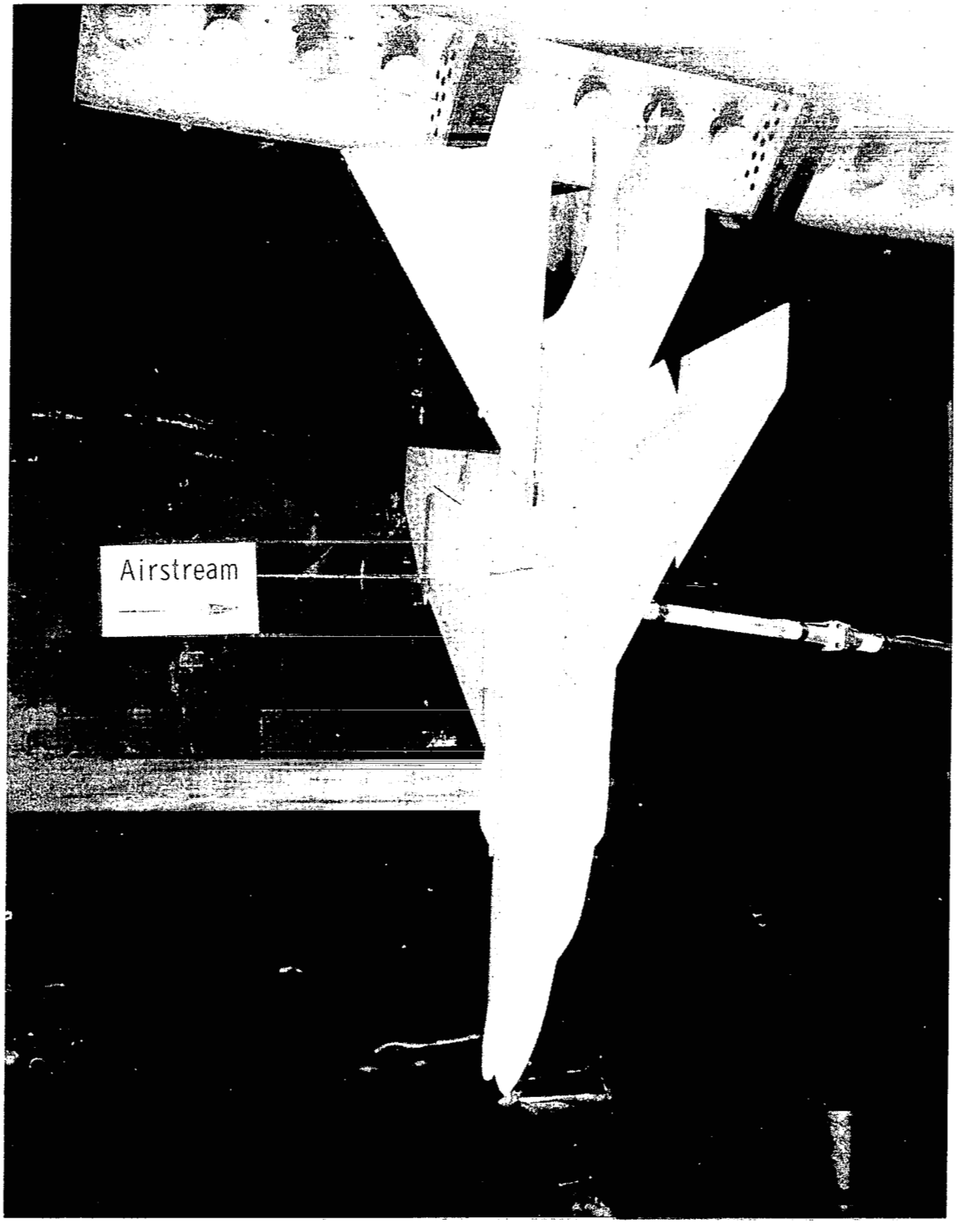

L-70-2810.1

Figure 15.- The 1/11-scale static model A equipped with a nondeployable ventral fin mounted in a low-speed wind tunnel.

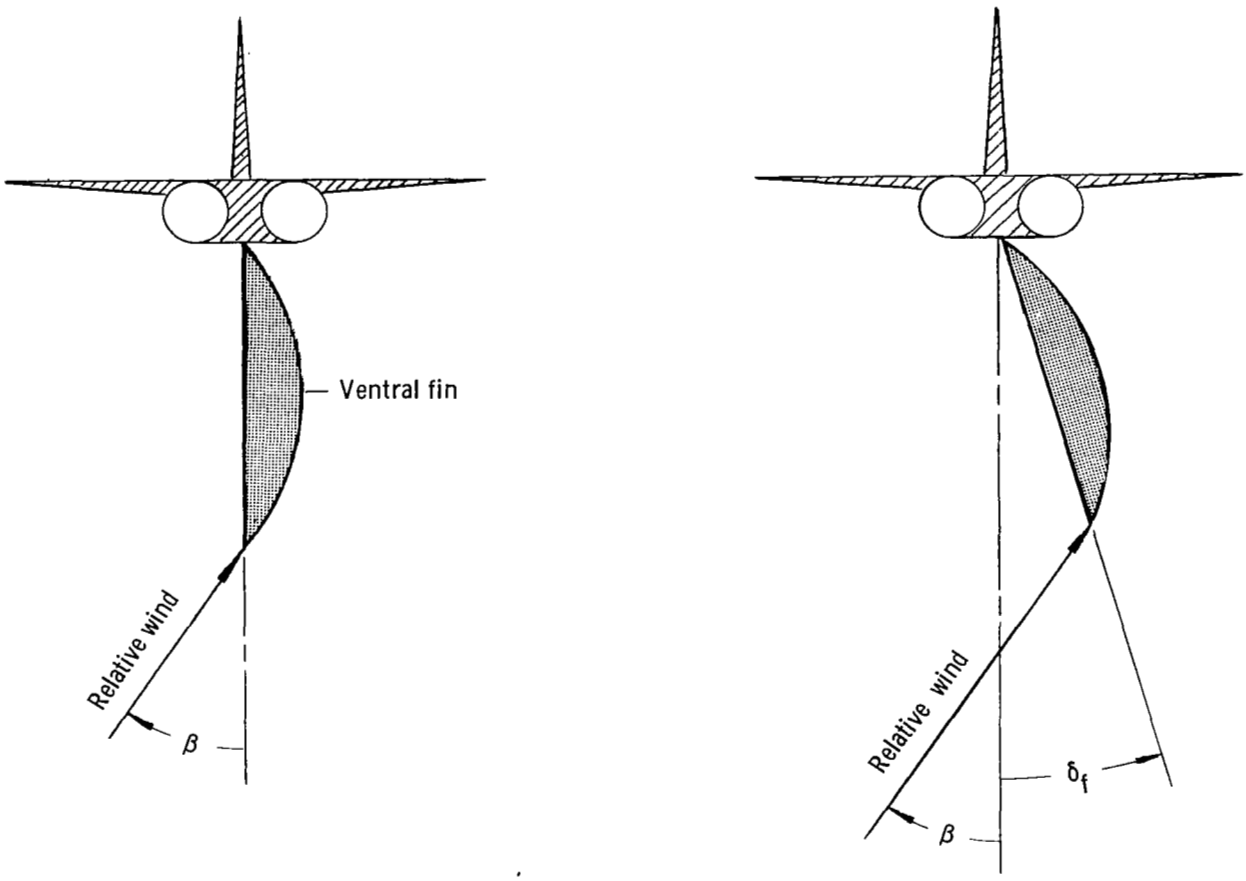

(a) Ventral fin undeflected.

(b) Ventral fin deflected.

Figure 16.- Illustration of relative wind direction at rear of model and curvature of ventral-fin fabric.

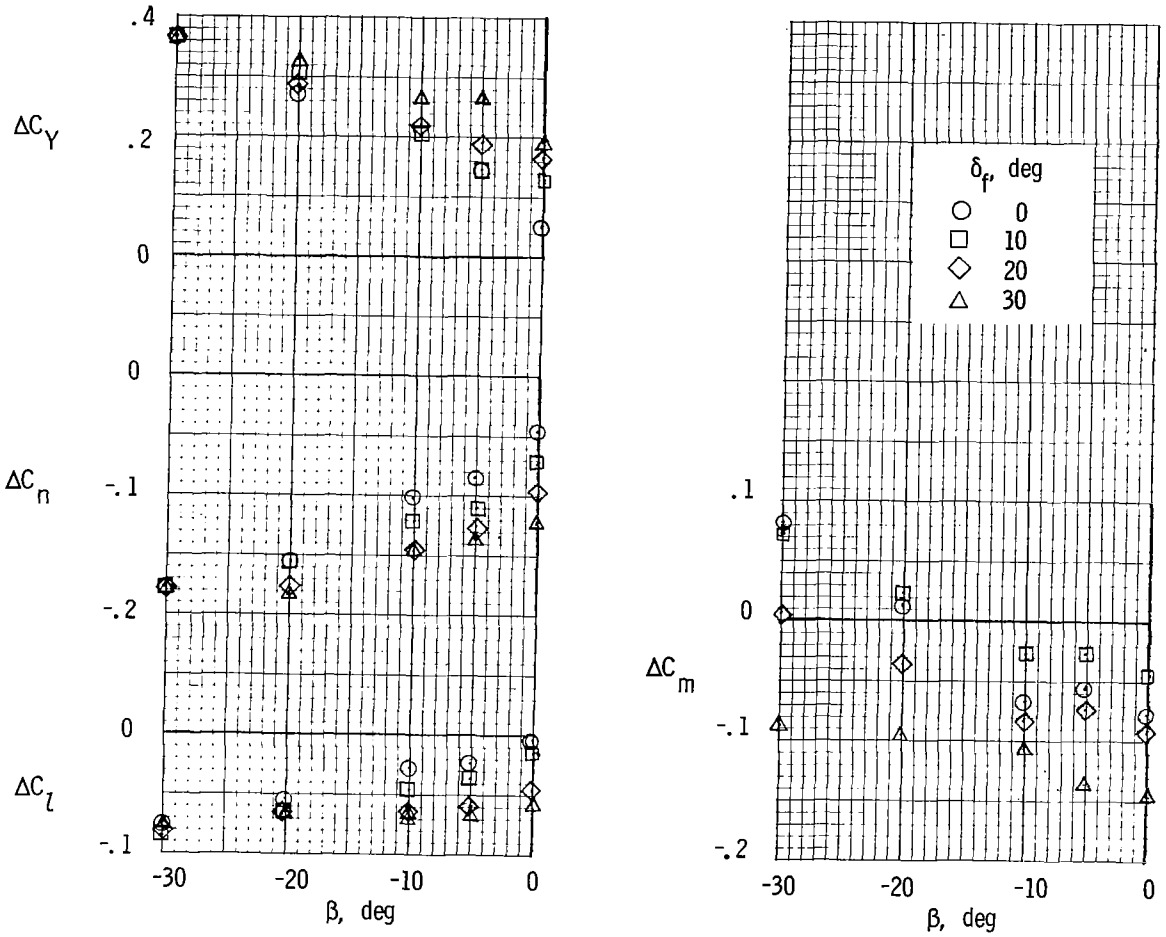

Figure 17.- Effect of deflections of large single ventral fin on incremental values of lateral and longitudinal coefficients for various angles of sideslip of static model A. $\alpha_s = 85^o$; position I.

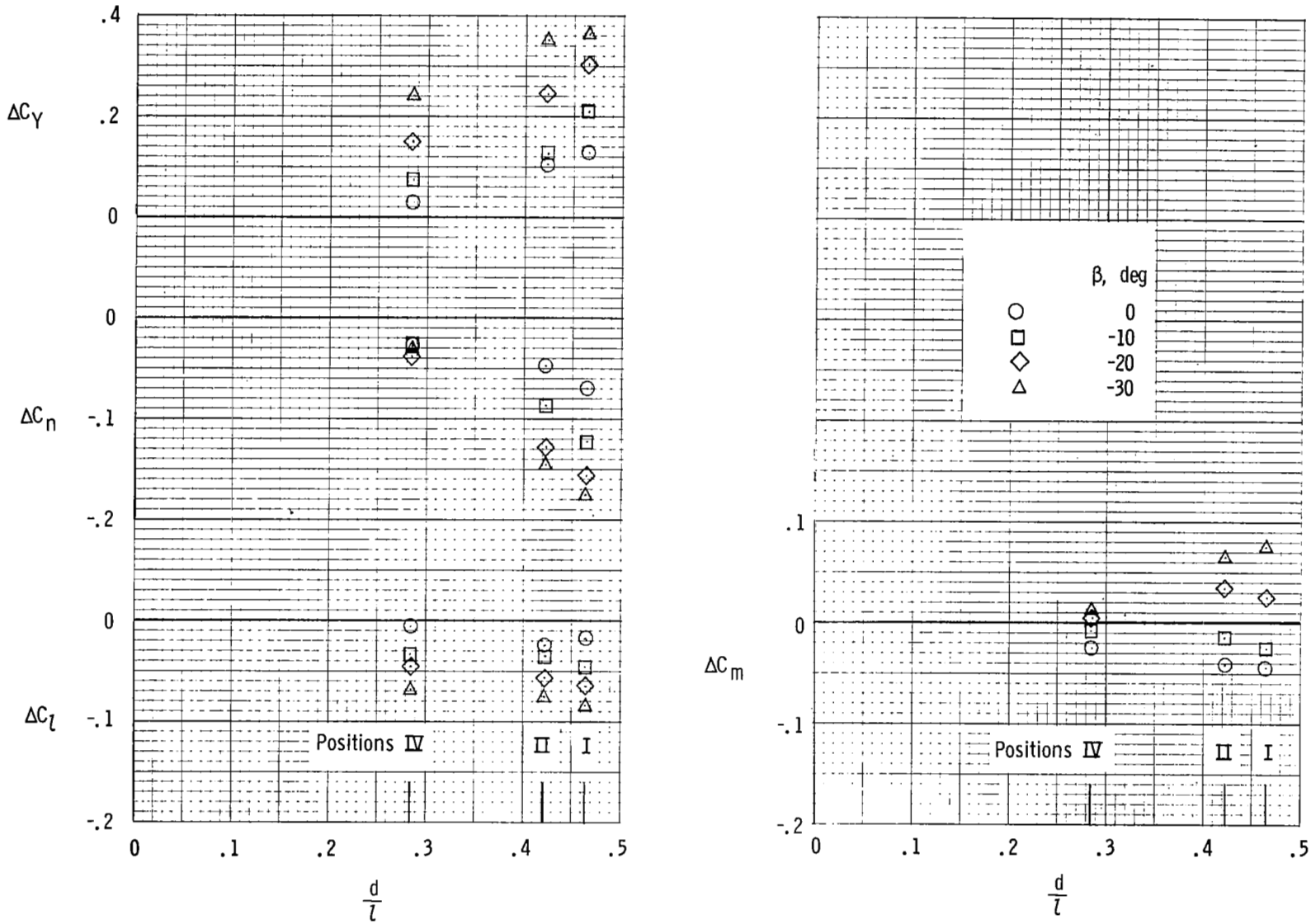

Figure 18.- Effect of longitudinal location of large ventral fin on incremental values of lateral and longitudinal coefficients for various angles of sideslip of static model A. $\alpha_s = 85^o$; $\delta_f = 10^o$.

A motion-picture film supplement L-1103 is available on loan. Requests will be filled in the order received. You will be notified of the approximate date scheduled.

The film (16 mm, 4 min, color, silent) shows the effects of various ventral-fin configurations, deflections, and locations on the spin-recovery characteristics of dynamic models A and B. Both satisfactory and unsatisfactory spin recoveries are shown.

Film supplement L-1103 is available on request to:

NASA Langley Research Center
Att: Photographic Branch, Mail Stop 171
Hampton, Va. 23365

CUT

Date _____

Please send, on loan, copy of film supplement L-1103 to TN D-6509.

_____
Name of organization

_____
Street number

_____
City and State Zip code

Attention: Mr. _____
Title _____

"The aeronautical and space activities of the United States shall be conducted so as to contribute . . . to the expansion of human knowledge of phenomena in the atmosphere and space. The Administration shall provide for the widest practicable and appropriate dissemination of information concerning its activities and the results thereof."

—NATIONAL AERONAUTICS AND SPACE ACT OF 1958

NASA SCIENTIFIC AND TECHNICAL PUBLICATIONS

TECHNICAL REPORTS: Scientific and technical information considered important, complete, and a lasting contribution to existing knowledge.

TECHNICAL NOTES: Information less broad in scope but nevertheless of importance as a contribution to existing knowledge.

TECHNICAL MEMORANDUMS: Information receiving limited distribution because of preliminary data, security classification, or other reasons.

CONTRACTOR REPORTS: Scientific and technical information generated under a NASA contract or grant and considered an important contribution to existing knowledge.

TECHNICAL TRANSLATIONS: Information published in a foreign language considered to merit NASA distribution in English.

SPECIAL PUBLICATIONS: Information derived from or of value to NASA activities. Publications include conference proceedings, monographs, data compilations, handbooks, sourcebooks, and special bibliographies.

TECHNOLOGY UTILIZATION PUBLICATIONS: Information on technology used by NASA that may be of particular interest in commercial and other non-aerospace applications. Publications include Tech Briefs, Technology Utilization Reports and Technology Surveys.

Details on the availability of these publications may be obtained from:

SCIENTIFIC AND TECHNICAL INFORMATION OFFICE

NATIONAL AERONAUTICS AND SPACE ADMINISTRATION

Washington, D.C. 20546